Integrated Evaluation of Reliability and Stability of Power Systems

Mohammed Benidris, *Member, IEEE,* Joydeep Mitra, *Senior Member, IEEE,* and Chanan Singh, *Fellow, IEEE*

***Abstract*—This paper investigates the impacts of transient instability on power system reliability. Traditionally, composite system reliability evaluation has been performed based on steady-state estimation of load curtailments; system dynamics have often been ignored, mostly due to computational complexity. In this paper, three probabilistic transient stability indices are proposed to assess system robustness against dynamic contingencies and to account for system instability in computing reliability indices. A direct method is utilized for transient stability assessment based on computing the energy margin of the system under fault events (energy margins measure the ability of a system to withstand contingencies). Energy margins along with the probability of occurrences of the events are used to update the probabilistic transient stability indices. The dependencies of reliability and stability indices on the fault clearing time are also evaluated. This method is applied on the reduced Western Electricity Coordinating Council and the New England 39 bus test systems. The results indicate the importance of considering the effect of stability in reliability evaluation.**

***Index Terms*—Reliability, transient stability, direct methods.**

I. Introduction

MODERN power systems are increasingly being operated close to their stability limits due to the increase in the penetration level of renewable energy sources, market forces, and recent advances in computation and communication technologies. In composite system reliability evaluation, following a contingency, faulted components are assumed to be disconnected from the grid immediately and the system is assumed to return to a stable state with suitable generation rescheduling for minimum load curtailments. Although the generation rescheduling optimization problem may converge to a feasible solution representing a steady-state operating point, a stable transition to a post-fault Stable Equilibrium Points (SEP) is not guaranteed. Therefore, transient stability assessment is an important factor that should be considered in evaluating the reliability of a given system. However, transient stability assessment is computationally expensive and for this reason system dynamics are often ignored in reliability evaluation.

Power systems may evolve along any of numerous possible trajectories after occurrence of potentially destabilizing contingencies. The computational challenge of performing time-domain simulation of every or even a selected set of probable trajectories has prohibited the inclusion of transient stability analysis in the applications that require repetitive computations such as reliability assessment. More recently, however, there have been theoretical developments that potentially enables determination of system stability with low computation burden. These methods are predominantly based on direct methods, such as Lyapunov and energy function methods. Direct methods recursively filter a set of possible contingencies into *stable*, *potentially unstable*, and *undetermined* sets. In other words, direct methods screening tools selectively exclude stable contingencies and perform detailed analyses on the undertermined and potentially unstable contingencies [1]–[6]. For instance, three levels of filtering each of which has inertial and post-inertial time frames has been proposed in [1], [2]. The filtering process is applied along the solution sequence toward controlling unstable equilibrium points (controlling UEPs). Transient stability screening for online applications using the Boundary of stability region based Controlling Unstable equilibrium point method (BCU method) has been proposed in [3]. Six classifiers are used to omit stable and mild contingencies and pass undertermined contingencies for further detailed analyses. Subsequently, the authors of [3] introduced improvements to the classifiers in [4]. One of the improvements is adding an islanding mode classifier. A screening tool based on direct methods that utilizes a homotopy-based approach has been proposed in [7], [8].

Time-domain simulation may be performed to evaluate potentially unstable and undetermined contingencies. However, direct methods have proved to be effective in reducing the volume of contingencies that require detailed analysis using time-domain simulations, and thereby made it possible to screen and compute dynamic contingencies in real-time. Thus, one saves significant computation time without compromising accuracy. If the initial condition does not belong to any region of attraction (ROA) or belongs to the ROA of an unstable solution or belongs to the ROA of an unrealizable equilibrium (e.g. solution in complex domain), then time domain simulation may be required to determine system trajectories. However, even under such a circumstance it is noted that the time-domain simulation can be avoided by determining a suitable initial point. Thus, the extent to which time-domain simulations are required may not be significant.

The effect of transient instability on power system reliability has been introduced in [9]–[11]. The work presented in [9] evaluates the effect of transient instability on power system reliability using time-domain simulation which is time consuming. On the other hand, the work presented in [10] evaluates the stability of the system based on the potential

M. Benidris is with the Department of Electrical and Biomedical Engineering, University of Nevada, Reno, Reno, NV 89557 USA, e-mail: mbenidris@unr.edu.

J. Mitra is with the Department of Electrical and Computer Engineering, Michigan State University, East Lasing, MI, 48823 USA, e-mail: mitraj@msu.edu.

C. Singh is with the Department of Electrical Engineering, Texas A&M University, College Station, TX 77843, USA, e-mail: singh@ece.tamu.edu.

This work was supported by the U.S. Department of Energy under Award DE-OE0000625.

energy boundary surface (PEBS) method. However, the accuracy of the PEBS method strongly relies on the choice of the critical machine, and thus it may produce inaccurate results [12]. Further, the work presented in [9], [10] do not consider system robustness against fault events which is an important factor in planning studies. The work presented in [11] is based on determining the probabilistic fault critical clearing times for system components which is computationally expensive even for small systems as concluded by the authors, requires statistical data for protection malfunctions, and does not count for variations in system conditions. Also, stationary probabilities instead of chronological representation of system events are used which do not capture the sequence of faults if more than one component is failed. In other words, only first order contingencies are considered.

The work presented in this paper evaluates both the effect of transient stability on power system reliability and the degree of system stability using the concept of direct methods and the controlling UEP. The proposed investigation of the impact of transient stability on power system reliability adds another dimension toward realistic modeling of power system reliability evaluation. Three probabilistic transient stability indices are introduced: (1) expected transient instability index which provides an evaluation of the system instability, (2) expected transient stability robustness index which measures the ability of a system to withstand fault events, and (3) the expected system risk of instability index which measures the risk of a system being unstable following fault events. Also, four reliability indices are evaluated, namely, loss of load probability, frequency, and duration, and expected power not supplied. The effect of the fault clearing time on the reliability and stability indices is also evaluated. Monte Carlo next event method is used in determining the reliability and stability indices. The results of the effect of transient stability on power system reliability and the robustness of power systems against disturbances are provided.

The remainder of the paper is organized as follows. Section II presents models of power system networks in reliability studies and power system reliability indices. Section III describes the transient stability assessment approach using direct methods and a homotopy-based method. Section IV introduces the proposed transient stability indices. Section V shows the implementation of the proposed method on two test systems. Section VI provides concluding remarks.

II. Network Modeling and Reliability Analysis

This section describes modeling of power system networks for minimum load curtailment using linear programming and the evaluation of the reliability indices. Linear programming has been commonly used in evaluating the reliability indices of composite systems. The objective function is minimum load curtailment. For every system state, if load curtailment is unavoidable, an optimal redispatch algorithm minimizes the amount of load to be shed.

A. Linear Programming for Minimum Load Curtailment

Optimal redispatch algorithms consider two types of constraints: equality and inequality constraints. The equality constraints represent the power balance at the system buses and the inequality constraints represent the equipment capability limits (generation and transmission capacities). The linear programming formulation of the network with the DC power flow model is given in (1) and (2) [13].

$$LC = \min\left(\sum_{i=1}^{N_b} C_i\right). \tag{1}$$

Subject to:

$$\begin{aligned} \widehat{B}\theta + G + C &= D \\ G &\leq G^{max} \\ b\widehat{A}\theta &\leq F_f^{max} \\ -b\widehat{A}\theta &\leq F_r^{max} \\ G, C &\geq 0 \\ \theta &\quad \text{unrestricted} \end{aligned} \tag{2}$$

where N_t is the number of lines, N_b is the number of buses, LC is the amount of load curtailment, b is the susceptance matrix of transmission line, $\widehat{B}$ is the augmented node susceptance matrix, $\widehat{A}$ is the element-node incidence matrix, G^{max} is the vector of maximum available generation, C is the vector of bus load curtailments, θ is the vector of bus voltage angles, D is the vector of bus load, G is the solution vector of the generation at buses, and F_r^{max} and F_f^{max} are the vectors of reverse and forward flow capacities of lines, respectively.

B. Calculation of Reliability Indices

Simulation methods have been commonly implemented in reliability evaluation of power systems. In this work, the Monte Carlo next event method [14] is used in sampling system states X (for both reliability and stability studies) and evaluating the reliability and stability indices. Monte Carlo next event is used here due to the following reasons: (a) Monte Carlo state duration method is computationally expensive and it requires large memory storage, and (b) Monte Carlo state sampling method do not provide the sequence of events which introduces a difficulty in evaluating transient stability indices.

In estimating the reliability indices, the expected values are used to evaluate the indices. If an index is denoted by η, the expected value of the index is calculated as follows.

$$\hat{\eta} = E\left[\eta\right], \tag{3}$$

where $E\left[\bullet\right]$ is the expectation operator.

1) Loss of Load Probability (LOLP) Index: The probability of failure of the system to meet the demand is expressed by the LOLP index and is calculated using (4).

$$q = \sum_{i=1}^{n_f} P\left\{x_i : x_i \in X_f\right\}, \tag{4}$$

where q denotes the LOLP index, X_f is the set of failure states ($X_f \subset X$), X is the set of all states, x_i is the system state i, $P\left\{x_i : x_i \in X_f\right\}$ is the probability of the system being in state x_i, and n_f is the number of failure states.

Using Monte Carlo simulations, sampled states are evaluated and the failure probability index, q, is updated. In this

regard, the estimated value of the LOLP index, $\hat{q}$, is calculated using Monte Carlo simulation as follows.

$$\hat{q} = \frac{1}{T}\sum_{i=1}^{N}\vartheta_i, \tag{5}$$

where T is the sum of the durations of all sampled system states, N is the number of samples, and ϑ_i can be expressed as follows.

$$\vartheta_i = \begin{cases}\tau_i, & \text{if } x_i \in X_f\\ 0, & \text{otherwise}\end{cases} \tag{6}$$

where τ_i is the time duration of state x_i.

2) Calculation of the Expected Power Not Supplied (EPNS) Index: The EPNS index measures the expected load that will be shed in cases of failure states. The EPNS index is calculated using (7) where ρ denotes the EPNS index.

$$\rho = \sum_{i=1}^{n_f} P\left\{x_i : x_i \in X_f\right\} \times LC\left\{x_i : x_i \in X_f\right\}, \tag{7}$$

where $LC\left\{x_i : x_i \in X_f\right\}$ is the amount of load curtailment of state x_i.

Using Monte Carlo simulations, sampled states are evaluated and the EPNS index, ρ, is updated based on the amount of load curtailment. The estimated EPNS index, $\hat{\rho}$, is calculated using Monte Carlo simulation as follows.

$$\hat{\rho} = \frac{1}{T}\sum_{i=1}^{N}\psi_i, \tag{8}$$

where ψ_i represents the amount of curtailment and is expressed as follows.

$$\psi_i = \begin{cases}\tau_i \times LC_i, & \text{if } x_i \in X_f\\ 0, & \text{otherwise}\end{cases} \tag{9}$$

3) Calculation of Frequency and Duration Indices: Frequency and duration indices provide measures for how often and how long a load is curtailed. It is worth mentioning here that calculation of frequency and duration indices using Monte Carlo state sampling method, for example, is not a straightforward process as is for probability and energy indices; some manipulations to the Monte Carlo state sampling method have been introduced in [15]–[17]. However, Monte Carlo next event method is adopted in this work due to this reason and the reasons mentioned in section II-B. The estimated LOLF index ($\hat{\phi}$) is calculated as follows.

$$\hat{\phi} = \frac{1}{T}\sum_{i=1}^{N}\varphi_i \times 8760, \tag{10}$$

where φ_i is a binary indicator for the transitions between success and failure states which is expressed as follows.

$$\varphi_i = \begin{cases}1, & \text{if } x_{i-1} \in X_s \text{ and } x_i \in X_f\\ 0, & \text{otherwise}\end{cases} \tag{11}$$

where X_s is the set of success states (i.e., $X_s \subset X$).

The expected fault duration index is defined in terms of the LOLD index which is calculated using (12) where $\hat{\tau}$ is the estimated value of the LOLD index.

$$\hat{\tau} = \frac{\hat{q}}{\hat{\phi}}. \tag{12}$$

Through sampling process, success states are reevaluated using transient stability analysis as explained in section III. If the transition is unstable, reliability and stability indices are updated; otherwise, it is classified as a stable transition. The effect of transient instability is not considered in evaluating the static reliability indices. On the other hand, the effect of transient instability is included in the dynamic reliability indices (as shown in section III) so that if failure of a system component causes instability, the duration of the state is included in the LOLP index, the amount of outage power is included in the EPNS index, and the transition failure is included in the LOLF index.

III. Transient Stability Assessment

Power system transient stability model (in the time horizon of milliseconds) and the energy function are presented in this section.

A. The Dynamical Model

For an n-generator system, the transient stability model of the generators for a uniform damping with respect to the center of inertia (COI) can be defined as follows [18].

$$\dot{\tilde{\delta}}_i = \tilde{\omega}_i, \tag{13}$$

$$\dot{\tilde{\omega}}_i = \frac{1}{M_i}\left(P_{mi} - P_{ei}\right) - \frac{1}{M_T}P_{COI} - \lambda_d\,\tilde{\omega}_i, \tag{14}$$

where P_{ei} is the electrical power output of machine i, P_{mi} is the mechanical input of machine i, δ_i and ω_i are power angle and speed of machine i respectively, M_i is the inertia constant of machine i, and P_{COI} is the power associated with the COI reference frame, $\tilde{\delta}_i = \delta_i - \delta_o$, $\tilde{\omega}_i = \omega_i - \omega_o$, $\delta_o = \frac{1}{M_T}\sum_{i=1}^{n} M_i\delta_i$, $\omega_o = \frac{1}{M_T}\sum_{i=1}^{n} M_i\omega_i$, $M_T = \sum_{i=1}^{n} M_i$ and λ_d is the uniform damping constant.

The compact form of the system of (13) and (14) can be presented as follows.

$$\dot{x} = \mathrm{g}(x, t), \tag{15}$$

where x is dynamic state vector of generating units and $\dot{x}$ is time-derivative of x.

The electrical power of machine i is given as follows.

$$P_{ei} = \sum_{j=1}^{n} E_i E_j \left[G_{ij}\cos\left(\tilde{\delta}_i - \tilde{\delta}_j\right) + B_{ij}\sin\left(\tilde{\delta}_i - \tilde{\delta}_j\right)\right] \tag{16}$$

where B_{ij} and G_{ij} are the susceptance and conductance matrices of the network model and E_i is the internal voltage magnitude of machine i.

The power of the center of inertial, P_{COI}, is computed as follows.

$$P_{COI} = \sum_{i=1}^{n} P_{mi} - \sum_{i=1}^{n}\sum_{j=1}^{n} E_i E_j \left[G_{ij}\cos\left(\tilde{\delta}_i - \tilde{\delta}_j\right) + B_{ij}\sin\left(\tilde{\delta}_i - \tilde{\delta}_j\right)\right]. \tag{17}$$

B. The Energy Function

In transient stability analysis, the energy function is used in screening and computing the exit point (EP) which is in turn is used to generate a sequence of steps to calculate the controlling UEP. The energy function associated with the model of (15) is given in (18) [19], [20]. The first term of (18) is the kinetic energy function and the last two terms are the potential energy function.

$$V = \frac{1}{2}\sum_{i=1}^{n} M_i\tilde{\omega}_i^2 - \sum_{i=1}^{n} P_i\left(\tilde{\delta}_i - \tilde{\delta}_i^s\right) - \sum_{i=1}^{n-1}\sum_{j=i+1}^{n}\left[C_{ij}\left(\cos\tilde{\delta}_{ij} - \cos\tilde{\delta}_{ij}^s\right) - I_{ij}\right], \quad (18)$$

where

$$P_i = P_{mi} - E_i^2 G_{ii},$$

and I_{ij} is the absorbed energy in the transfer conductances. The term I_{ij} can be expressed as follows.

$$I_{ij} = \int_{\tilde{\delta}_i^s+\tilde{\delta}_j^s}^{\tilde{\delta}_i+\tilde{\delta}_j} D_{ij}\cos\tilde{\delta}_{ij}\; d\left(\tilde{\delta}_i + \tilde{\delta}_j\right). \quad (19)$$

The integral term of (19) depends on the system trajectory which is not known in advance. Several methods have been suggested in the literature to approximate this term. In this paper, the method suggested by [19] is used which can be given as follows.

$$I_{ij} = D_{ij}\frac{\tilde{\delta}_i + \tilde{\delta}_j - \tilde{\delta}_i^s - \tilde{\delta}_j^s}{\tilde{\delta}_i - \tilde{\delta}_j - \tilde{\delta}_i^s + \tilde{\delta}_j^s}\left[\sin\tilde{\delta}_{ij} - \sin\tilde{\delta}_{ij}^s\right]. \quad (20)$$

The approximation of the path dependent term I_{ij} usually causes imprecise determination of the EP. However, using the homotopy method, accurate EPs are not necessary in finding the controlling UEPs.

C. Calculation of the Controlling UEP

Determination of the controlling UEPs is pivotal in determining the critical energy which is used to assess the stability of the system. A state vector x is called an equilibrium point x^* of the dynamic system represented in (15) if $\dot{x} = 0$. One of the unstable equilibrium points (UEP) of (15) is the controlling UEP. However, the controlling UEP is a unique UEP such that it is located in the direction of the post-fault trajectory. Mathematically, a controlling UEP is a UEP with a property that its stable manifold, $W^s(X_{co})$, intersects with the EP [12], [19], [21], [22] as shown in Fig. 1. The EP is a point at which the sustained fault-on trajectory $(\delta(t), \omega(t))$ intersects with the stability boundary of the post-fault SEP. Mathematically, the EP is determined by the first local maximum value of the potential energy (the last two terms of (18)) of the post-fault network.

The terms used in Fig. 1 are defined as follows: MGP is the minimum gradient point, EP is the exit point, $A(X_s)$ is the ROA of the post-fault SEP (X_s), X_{co} is a controlling UEP, $R(X_{co})$ is the convergence region of a controlling UEP,

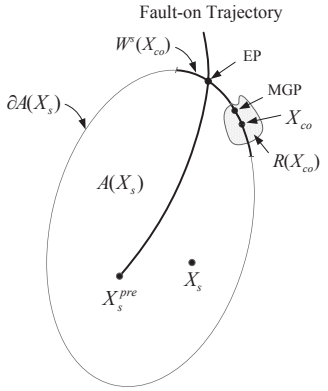

Fig. 1. Region of stability and the controlling UEP [21].

$\partial A(X_s)$ is the boundary of the ROA, X_s^{pre} is the pre-fault SEP, and $W^s(X_{co})$ is the stable manifold. The MGP is numerically defined as the first minimum value of the norm of the vector field of the post-fault trajectory of (15) [21].

The convergence region can be defined as follows: starting from an initial point, an iterative numerical method finds the desired solution if the starting point is located inside the region of convergence of the solution, and it fails to find the desired solution if the initial point is located outside the region of convergence. However, the region of convergence of a controlling UEP can be fractal and it varies, in terms of its size and shape, according to the used numerical method [21]. Thus, if the initial point is not inside the convergence region of the controlling UEP, iterative methods will no converge to the relevant controlling UEP. In other words, to ensure convergence, the initial point must be sufficiently near to the controlling UEP.

Time-domain simulations have been commonly used in simulating the fault-on trajectory to determine the EP and then the MGP. The MGP is used as an initial point to generate a sequence of solution steps toward the controlling UEP [12], [22]–[27]. Consequently, the reliability of determining the controlling UEP relies strongly on the quality of the calculated MGP [22]–[24], [27], [28]. However, an inaccuracy in computing the EP could cause difficulty in determining the relevant MGP. Also, determining an accurate EP is computationally expensive and interpolation methods have been to used upon locating EPs within certain ranges. Therefore, a numerical inaccuracy in determining the EP will probably lead to failure of iterative methods to compute the controlling UEP.

In detecting the EP, most of the available methods simulate the fault-on trajectory using an adaptable step size until the EP is bounded between two time points. A more accurate EP is then detected by using numerical tools such as the golden section and linear/quadratic interpolations. Upon discovering a more accurate EP, the MGP is computed by simulating the post-fault trajectory. The MGP is then used as an initial point to calculate the controlling UEP. Thus, it is obvious that detecting the EP and determining the MGP is computationally involved. Also, the accuracy of finding the EP and the MGP is a major factor in computing the controlling UEP.

In this work, a homotopy-based method is used in computing the controlling UEP to overcome the requirement of

computing the MGP. Also, the homotopy-based method does not require accurate EPs. Homotopy-based methods are known to be globally convergent and are reliable in finding the solutions [29]–[32]. The homotopy-based method is explained in following section.

D. Homotopy-Based Method

Finding the equilibrium points of (15) have been based on iterative methods such as Newton methods. In this work, the homotopy-based method is used to compute the controlling UEPs of (15). The use of homotopy-based methods in computing the controlling UEPs was developed by the authors in [33]. We have found that the proposed homotopy based method is robust, reliable, and efficient in calculating the controlling UEP. Also, homotopy methods are not sensitive to the initial points. Though the rigorous derivation will not be reproduced here; the homotopy-based method is explained by means of simple arguments to derive expressions for the probabilistic stability indices.

Although homotopy-based methods are known to be reliable in calculating equilibrium points, they are intrinsically slow because these methods map the trajectory of the solution from a known solution to the desired solution. In this paper, the homotopy-based method is used with EPs as the initial points to find controlling UEPs. Therefore, using approximate EPs rather than determining accurate EPs, as is common practice in computing the controlling UEP, and avoiding the computational burden in finding MGPs, the intrinsic low speed of computation of homotopy-based approaches is compensated.

Homotopy is a continuation method to determine the roots of non-linear systems such as (15). The basic concept of the homotopy-based methods is that they determine solutions based on path continuation. The mapping starts at a known solution, x^0, (i.e., $G(x^0) = 0$) as shown in (21) which is the most widely homotopy function used in the literature.

$$H(x, \lambda) = \lambda F(x) + (1 - \lambda)G(x) = 0, \tag{21}$$

where λ is the mapping factor. The solution starts at $\lambda = 0$ and then λ is incrementally increased along the mapping process until $\lambda = 1$, i.e., $H(x, 1) = F(x)$ and $H(x, 0) = G(x)$.

In general, the function $G(x)$ is arbitrarily chosen as long as its solution is known. However, Newton Homotopy is the most widely used function which is given in (22).

$$G(x) = F(x) - F(x^0), \tag{22}$$

where x^0 is initial point. Thus, the homotopy function of (21) can be expressed as follows.

$$H(x, \lambda) = F(x) - (1 - \lambda)F(x^0) = 0. \tag{23}$$

In this paper, Newton homotopy is used to compute post-fault SEPs and controlling UEPs of the tested systems by which numerical problems in computing post-fault SEPs and controlling UEPs are avoided. The $F(x)$ function represents the dynamical model of the system as given in (15) and x^0 is the EP.

It should be noted that in applying homotopy methods, the direction of the search (forward or backward) for the solution is a major factor in computing the correct controlling UEPs. The direction of the search depends on the position of the EP with regard to the controlling UEP on the stability boundary. During the calculation process, the algorithm proceeds by assuming forward mapping for one homotopy iteration; if the solution diverges, the algorithm uses backward mapping.

E. Calculation of the Energy Margin

The energy margin is used to assess system transient stability for a particular contingency. Mathematically, the energy margin (ΔV) is the difference between the transient energy and the critical energy where both are determined from the energy function of (18); the transient energy is the value of the energy function at clearing time ($V_{c\ell}$) and the critical energy (V_{cr}) is the energy at the controlling UEP. The energy margin can be calculated using (24).

$$\Delta V = V_{cr} - V_{c\ell}. \tag{24}$$

If the energy margin is positive (i.e., $\Delta V > 0$), the system is deemed stable; otherwise, the system is deemed unstable under the designated contingency.

IV. Probabilistic Transient Stability Indices

To incorporate transient stability in power system reliability evaluation, this paper proposes three probabilistic stability indices to assess both system vulnerability and robustness against fault events which include initial contingencies and common mode failures. Direct methods in the form of the energy function are used to evaluate system stability for each contingency.

A. Expected Transient Instability Index

The expected transient instability (ETI) index provides a measure for the probability of the system being in an unstable state. Let α denote the ETI index which can be calculated as follows.

$$\alpha = \sum_{i=1}^{n_u} P\left\{x_{i-1,i} : x_{i-1,i} \in X_u\right\}, \tag{25}$$

where $P\left\{x_{i-1,i} : x_{i-1,i} \in X_u\right\}$ is the probability of the system being *unstable* while transitioning from state x_{i-1} to state x_i, x_i is the system new state, X_u is the set of unstable transitions ($X_u \subset X$), X is the set of all system states, and n_u is the number of unstable transitions.

A transition is considered unstable if the energy margin (EM) is less than zero, that is EM < 0. Using Monte Carlo next event sampling method, the estimated ETI index, $\hat{\alpha}$, is calculated as follows.

$$\hat{\alpha} = \frac{1}{T} \sum_{i=1}^{N} \gamma_i, \tag{26}$$

where γ_i is a duration function that can be calculated as follows.

$$\gamma_i = \begin{cases} \kappa_i, & \text{if } x_{i-1,i} \in X_u \\ 0, & \text{otherwise} \end{cases} \tag{27}$$

where κ_i is the residence time in a contingency that results in instability.

B. Expected Transient Stability Robustness Index

Expected transient stability robustness (ETSR) index measures the ability of a system to withstand fault events. Let β denote the ETSR index which can be calculated as follows.

$$\beta = \sum_{i=1}^{n_{st}} P\left\{x_{i-1,i} : x_{i-1,i} \in X_{st}\right\} \cdot \mathrm{EM}\left\{x_{i-1,i} : x_{i-1,i} \in X_{st}\right\} \tag{28}$$

where $P\left\{x_{i-1,i} : x_{i-1,i} \in X_{st}\right\}$ is the probability of the system being *stable* while transitioning from state x_{i-1} to state x_i, X_{st} is the set of stable transitions ($X_{st} \subset X$), n_{st} is the number of stable transitions and $\mathrm{EM}\left\{x_{i-1,i} : x_{i-1,i} \in X_{st}\right\}$ is the energy margin of a stable transition from state x_{i-1} to state x_i.

Using Monte Carlo next event method, the estimated ETSR index, $\hat{\beta}$, is calculated as follows.

$$\hat{\beta} = \frac{1}{T}\sum_{i=1}^{N} \varrho_i, \tag{29}$$

where ϱ_i is the energy margin of a stable transition ($x_{i-1,i} \in X_{st}$) which can be expressed as follows.

$$\varrho_i = \begin{cases} \mathrm{EM}, & \text{if } x_{i-1,i} \in X_{st} \\ 0, & \text{otherwise} \end{cases} \tag{30}$$

C. Expected System Risk of Instability Index

Expected system risk of instability (ESRI) index measures the risk of a system being unstable against fault events. Let ξ denote the ESRI index which can be calculated as follows.

$$\xi = \sum_{i=1}^{n_u} P\left\{x_{i-1,i} : x_{i-1,i} \in X_u\right\} \cdot \left|\mathrm{EM}\left\{x_{i-1,i} : x_{i-1,i} \in X_u\right\}\right| \tag{31}$$

where $\left|\mathrm{EM}\left\{x_{i-1,i} : x_{i-1,i} \in X_{st}\right\}\right|$ is the energy margin of an unstable transition from state x_{i-1} to state x_i.

Using Monte Carlo next event method, the estimated ESRI index, $\hat{\xi}$, is calculated as follows.

$$\hat{\xi} = \frac{1}{T}\sum_{i=1}^{N} \sigma_i, \tag{32}$$

where σ_i is the absolute value of the energy margin of an unstable transition ($x_{i-1,i} \in X_u$) which can be expressed as follows.

$$\sigma_i = \begin{cases} \left|\mathrm{EM}\right|, & \text{if } x_{i-1,i} \in X_u \\ 0, & \text{otherwise} \end{cases} \tag{33}$$

D. Reliability and Stability Assessment Procedure

In performing transient stability assessment using direct methods, numerical convergence problems may arise in calculating EPs, post-fault SEPs, and controlling UEPs. If a numerical problem is encountered, time-domain simulation is performed. The process of evaluating the reliability and probabilistic stability indices is shown in Fig. 2.

For every sampled state, optimal power flow is solved for minimum load curtailment. If the sampled state is a failure state (load curtailment is not avoidable), the reliability and stability indices are updated. If the sampled state is a success state (no load curtailment), the state is evaluated for transient instability. If it is unstable, reliability and stability indices are updated; otherwise, it is classified as a success state.

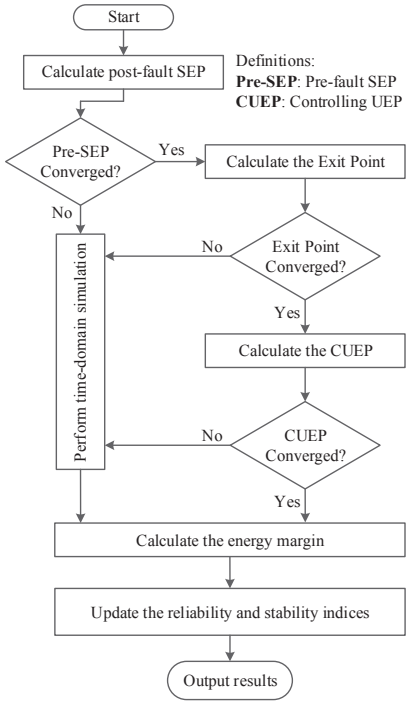

Fig. 2. The flowchart of the transient stability assessment procedure.

V. Case Studies

The reduced WECC 9 bus system and the NE 39 bus system are used to invesitigate the impacts of transient stability on power system reliability. The reduced WECC 9 bus system consists of 3 generators, 6 transmission lines, 3 transformers and 3 load buses [34]. The NE 39 bus system consists of 10 generators, 35 transmission lines, 12 transformers, and 19 load buses [35]. The reason of choosing these systems is because they have been extensively tested from transient stability perspective. The reliability data of the WECC system were taken from [9]. The mean time to failure (MTTF) and mean time to repair (MTTR) of the components of the NE 39 bus system are assumed as follows. The MTTFs of the transmission lines are assumed 4380 hours and the MTTRs are assumed 48 hours. The MTTFs of the transformers are assumed 87600 hours and the MTTRs are assumed 720 hours. The MTTFs and MTTRs data of the generators are given in Table I.

TABLE I
Generation reliability data of the NE 39 bus system

No.	Bus(es)	Unit size (MW)	MTTF (hour)	MTTR (hour)	Availability
1	30	350	2240	60	0.97391
2	31, 36, & 37	650	1520	80	0.95000
3	34	700	1550	80	0.95092
4	32, 33, & 35	750	1280	70	0.94815
5	38	900	1100	150	0.88000
6	39	1500*	12000	200	0.98361

*: represents the aggregation of a large number of generators.

Table II and Table III show the reliability indices as calculated with and without considering the effect of transient

stability for the WECC and the NE 39 bus systems respectively. These results provide a measure for static and dynamic estimations of the ability of the system to meet the demand. The amount of increase of these values in comparison with the case of not considering the transient instability reflects the contribution of dynamic instabilities.

TABLE II
STATIC AND DYNAMIC RELIABILITY ANNUALIZED INDICES OF THE WECC SYSTEM

	LOLP	EPNS MW	LOLF occ./yr	LOLD hour
Static	0.01575	1.42170	5.84841	23.59103
Static & dynamic	0.04092	1.93237	12.58263	28.48842

TABLE III
STATIC AND DYNAMIC RELIABILITY ANNUALIZED INDICES OF THE NE 39 BUS SYSTEM

	LOLP	EPNS MW	LOLF occ./yr	LOLD hour
Static	0.05063	22.53193	8.55621	51.83589
Static & dynamic	0.07773	31.56984	13.29079	51.23208

From Table II, static and dynamic indices of the WECC system, it can be seen that accounting for transient instabilities has more effect on the probability and frequency indices than the expected power not supplied index. The reason is that the static EPNS index of this system is relatively high and therefore including transient instabilities will have less effect on this index than other indices. The static EPNS index of this system is high because failure of a transformer, a transmission line, or a generator causes load curtailment.

From Table III, static and dynamic indices of the NE 39 bus system, it can be seen that accounting for transient instabilities has even effect on the LOLP, EPNS, and LOLF indices. There is a slight decrease in the LOLD index which can be related to fact that the rate of increase of the LOLF index is slightly larger than that of the LOLP index (the LOLD index is the ratio between the LOLP index and the LOLF index as shown in (12)). The reason is that this system has several parallel lines and interconnections and therefore failure of one component, except failure of the lines/transformers that result in separating the system into several subsystems, may not cause load curtailment.

TABLE IV
THE STABILITY INDICES OF THE WECC AND NE 39 BUS SYSTEMS

	ETI	ETSR	ESRI
WECC 9 bus system	0.02517	0.25603	0.10411
NE 39 bus system	0.05189	0.57240	0.11699

Table IV shows the stability indices of the tested systems. The critical clearing times of the WECC ranges from 210 ms to 330 ms. The critical clearing times of the NE 39 bus systems ranges from 0 ms (for the faulted components that cause islandings) to around 300 ms. The stability indices were calculated at a fault clearing time of 230 ms for the WECC system and 110 ms for the NE 39 bus system. The ETI index represents the probability of contributions of transient instabilities on load curtailments. The ETSR index represents robustness of the system against fault events which is calculated from the energy margins of the stable contingencies. The ESRI index represents the risk of the being unstable against fault events which is calculated from the energy margins of the unstable contingencies.

Systems that have high ETSR index are more robust to transient instabilities. On the other hand, systems with high values of ETI and ESRI indices are more vulnerable to transient instabilities. However, values of these indices depend strongly on the fault clearing time. In this work, the effect of fault clearing times on the stability and reliability indices of the NE 39 bus system is evaluated.

The amount of change in the reliability and stability indices of the NE 39 bus system against the fault clearing times are shown in Fig. 3 and Fig. 4 respectively. From these two figures, as the fault clearing time increases, the values of ETI and ESRI indices increase and the value of ETSR index decreases which is not surprising. However, an important observation is that if fault clearing times are less than 80 ms, the system maintains its robustness against transient instabilities. This observation is useful in determining the sensitivity of the system to fault clearing times.

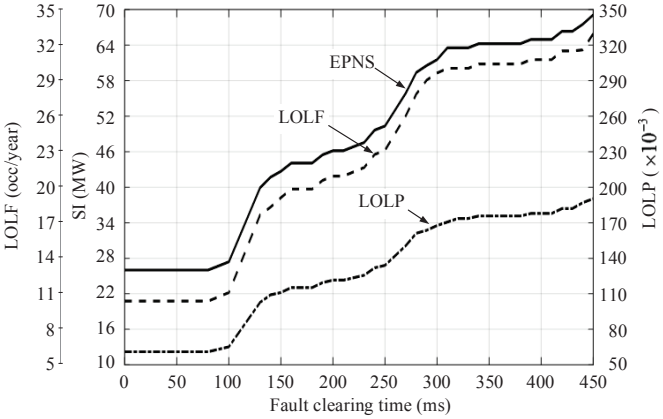

Fig. 3. Profiles of the *reliability* indices of the NE 39 bus system as functions of the clearing time where LOLP is the loss of load probability index, LOLF is the loss of load frequency index, and EPNS is expected power not supplied index.

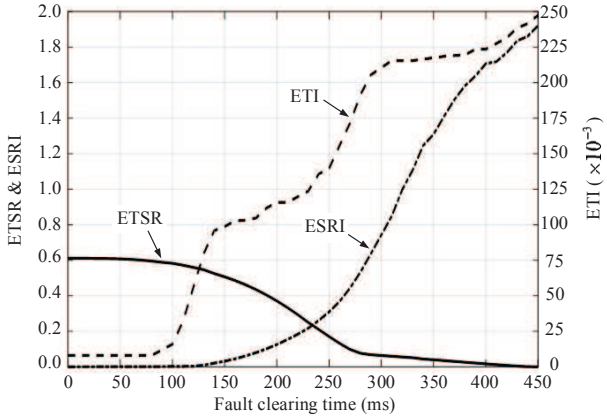

Fig. 4. Profiles of the *stability* indices of the NE 39 bus system as functions of the clearing time where ETI is the expected transient instability index, ETSR is the expected transient stability robustness index, and ESRI expected system risk of instability index.

VI. Conclusion

This paper has introduced a method to assess the effect of transient instability on power system reliability. Three probabilistic transient stability indices were introduced to measure the effect of transient stability on power system reliability which are: expected transient instability, expected transient stability robustness and the expected system risk of instability. Transient stability direct methods were used in assessing system stability, determining the energy margins and updating the stability and reliability indices. Also, power system reliability indices were evaluated for the cases considering and not considering the effect of transient instability. The effect of fault clearing times on power system reliability and stability indices was also evaluated. This method was applied on the reduced WECC and the NE 39 bus systems and the results showed that the effect of transient stability should not be ignored when evaluating reliability of the system. Also, the results of the stability indices can be used to measure system robustness against disturbances and the effect of fault clearing times on reliability and stability.

References

[1] "Analytical Methods for Contingency Selection and Ranking for Dynamic Security Analysis," Tech. Rep., EPRI TR-104352, Project 3103-03, Final Report, Siemens Energy & Automation Inc., Sept. 1994.

[2] V. Chadalavada, V. Vittal, G. C. Ejebe, G. D. Irissari, J. Tong, G. Pieper, and M. McMullen, "An On-Line Contingency Filtering Scheme for Dynamic Security Assessment," *IEEE Trans. Power Syst.*, vol. 12, no. 1, pp. 153–161, Feb. 1997.

[3] H.-D. Chiang, C. Wang, and H. Li, "Development of BCU Classifiers for On-Line Dynamic Contingency Screening of Electric Power Systems," *IEEE Trans. Power Syst.*, vol. 14, no. 2, pp. 660–666, May 1999.

[4] H.-D. Chiang, H. Li, J. Tong, and Y. Tada, "On-Line Transient Stability Screening of a Practical 14,500-Bus Power System: Methodology and Evaluations," in *High Performance Computing in Power and Energy Systems*, S. Khaitan and A. Gupta, Eds. Springer Heidelberg, 2013, pp. 335–358.

[5] D. Ernst, D. Ruiz-Vega, M. Pavella, P. Hirsch, and D. Sobajic, "A Unified Approach to Transient Stability Contingency Filtering, Ranking and Assessment," *IEEE Trans. Power Syst.*, vol. 16, no. 3, pp. 435–443, Aug. 2001.

[6] Y. Mansour, E. Vaahedi, A. Y. Chang, B. R. Corns, B. W. Garrett, K. Demaree, T. Athay, and K. Cheung, "B. C. Hydro's On-line Transient Stability Assessment (TSA): Model Development, Analysis and Post-processing," *IEEE Trans. Power Syst.*, vol. 10, no. 1, pp. 241–253, Feb. 1995.

[7] M. Benidris, N. Cai, and J. Mitra, "A Fast Transient Stability Screening and Ranking Tool," in *Proc. of the 8th Power Systems Computation Conference (PSCC)*, Wroclaw, Poland, Aug. 2014, pp. 1–6.

[8] J. Mitra, M. Benidris, and N. Cai, "Use of Homotopy-based Approaches in Finding Controlling Unstable Equilibrium Points in Transient Stability Analysis," in *Proc. of the 19th Power Systems Computation Conference (PSCC), (to appear)*, Genoa, Italy, June 2016, pp. 1–7.

[9] G. M. Huang and Y. Li, "Power System Reliability Indices to Measure Impacts Caused by Transient Stability Crises," in *Proc. of the IEEE Power Engineering Society Winter Meeting*, vol. 2, New York, NY, USA, Jan. 2002, pp. 766–771.

[10] A. M. Rei, A. M. Leite da Silva, J. L. Jardim, and J. Carlos de Oliveira Mello, "Static and Dynamic Aspects in Bulk Power System Reliability Evaluations," *IEEE Trans. Power Syst.*, vol. 15, no. 3, pp. 189–195, Feb. 2000.

[11] A. M. Leite da Silva, J. Endrenyi, and L. Wang, "Integrated Treatment of Adequacy and Security in Bulk Power System Reliability Evaluations," *IEEE Trans. Power Syst.*, vol. 8, no. 2, pp. 275–285, March 1993.

[12] H.-D. Chiang, F. F. Wu, and P. P. Varaiya, "A BCU Method for Direct Analysis of Power System Transient Stability," *IEEE Trans. Power Syst.*, vol. 9, no. 3, pp. 1194–1208, Aug. 1994.

[13] C. Singh and J. Mitra, "Composite System Reliability Evaluation Using State Space Pruning," *IEEE Trans. Power Syst.*, vol. 12, no. 1, pp. 471–479, Feb. 1997.

[14] C. Singh, T. Pravin, M. P. Bhavaraju, and M. Lauby, "A Monte Carlo Tool for Estimating Contingency Statistics," vol. 2, Sep. 1993, pp. 670–674.

[15] C. Singh, "Calculating the Time–specific Frequency of System Failure," *IEEE Trans. on Reliability*, vol. R-28, no. 2, pp. 124–126, June 1979.

[16] J. Mitra and C. Singh, "Pruning and Simulation for Determination of Frequency and Duration Indices of Composite Power Systems," *IEEE Trans. Power Syst.*, vol. 14, no. 3, pp. 899–905, Aug. 1999.

[17] A. C. G. Melo, M. V. F. Pereira, and A. M. Leite da Silva, "A Conditional Probability Approach to the Calculation of Frequency and Duration Indices in Composite Reliability Evaluation," *IEEE Trans. Power Syst.*, vol. 8, no. 3, pp. 1118–1125, Aug. 1993.

[18] A. A. Fouad and V. Vittal, *Power System Transient Stability Analysis using the Transient Energy Function Method*. Englewood Cliffs, NJ: Prentice-Hall, 1991.

[19] T. Athay, R. Podmore, and S. Virmani, "A Practical Method for the Direct Analysis of Transient Stability," *IEEE Trans. Power App. Syst.*, vol. PAS-98, no. 2, pp. 573–584, March 1979.

[20] A. A. Fouad and S. E. Stanton, "Transient Stability of a Multi-Machine Power System Part I: Investigation of System Trajectories," *IEEE Trans. Power App. Syst.*, vol. PAS-100, no. 7, pp. 3408–3416, July 1981.

[21] H.-D. Chiang, *Direct Methods for Stability Analysis of Electric Power Systems: Theoretical Foundation, BCU Methodologies, and Applications*. John Wiley & Sons, 2011.

[22] I. S. Nazareno, L. F. C. Alberto, and N. G. Bretas, "Problems in the Precise Determination of BCU's Controlling Unstable Equilibrium Points and PEBS's Exit Point Method in Real-time Transient Stability Analysis," in *Proc. IEEE/PES Trans. and Dist. Conf. Expo.: Latin America*, Nov. 2004, pp. 475–480.

[23] R. T. Treinen, V. Vittal, and W. Kliemann, "An Improved Technique to Determine the Controlling Unstable Equilibrium Point in a Power System," *IEEE Trans. Circuits Syst. I, Fundam. Theory Appl.*, vol. 43, no. 4, pp. 313–323, April 1996.

[24] L. Chen, Y. Min, F. Xu, and K.-P. Wang, "A Continuation-Based Method to Compute the Relevant Unstable Equilibrium Points for Power System Transient Stability Analysis," *IEEE Trans. Power Syst.*, vol. 24, no. 1, pp. 165–172, Feb. 2009.

[25] J. Lee and H.-D. Chiang, "Convergent Regions of the Newton Homotopy Method for Nonlinear Systems: Theory and Computational Applications," *IEEE Trans. Circuits Syst. I, Fundam. Theory Appl.*, vol. 48, no. 1, pp. 51–66, Jan. 2001.

[26] A. Llamas, J. De La Ree Lopez, L. Mili, A. G. Phadke, and J. S. Thorp, "Clarifications of the BCU Method for Transient Stability Analysis," *IEEE Trans. Power Syst.*, vol. 10, no. 1, pp. 210–219, Feb. 1995.

[27] A. Xue, S. Mei, and B. Xie, "A Comprehensive Method to Compute the Controlling Unstable Equilibrium Point," in *Proc. of 3rd International Conference on Electric Utility Deregulation and Restructuring and Power Technologies*, April 2008, pp. 1115–1120.

[28] J. Lee, "An Optimization-driven Framework for the Computation of the Controlling UEP in Transient Stability Analysis," *IEEE Trans. Autom. Control*, vol. 49, no. 1, pp. 115–119, Jan. 2004.

[29] D. Wolf and S. Sanders, "Multi-Parameter Homotopy Methods for Finding DC Operating Points of Nonlinear Circuits," in *Proc. of the IEEE International Symposium on Circuits and Systems*, vol. 4, Chicago, IL, USA, May 1993, pp. 2478–2481.

[30] L. T. Watson, "Globally Convergent Homotopy Methods: a Tutorial," *Applied Mathematics and Computation*, vol. 31, pp. 369–396, 1989.

[31] R. Kalaba and L. Tesfatsion, "Solving Nonlinear Equations by Adaptive Homotopy Continuation," *Applied Mathematics and Computation*, vol. 41, no. 2, pp. 99–115, 1991.

[32] J. C. Alexander and J. A. Yorke, "The Homotopy Continuation Method: Numerically Implementable Topological Procedures," *Transactions of the American Mathematical Society*, vol. 242, pp. 271–284, 1978.

[33] J. Mitra, M. Benidris, and N. Cai, "Tool Employing Homotopy-Based Approaches in Finding the Controlling Unstable Equilibrium Points in the Electric Power Grid," Patent US 20 160 041 232, Feb. 11, 2016. [Online]. Available: http://www.freepatentsonline.com/y2016/0041232.html

[34] University of Washington. Power Systems Test Case Archive. [Online]. Available: http://www.ee.washington.edu/research/pstca

[35] Illinois Center for a Smarter Electric Grid. 10-machine New-England Power System. [Online]. Available: http://icseg.iti.illinois.edu/ieee-39-bus-system/